JOURNAL OF GEOPHYSICAL RESEARCH, VOL. 115, B07413, doi:10.1029/2009JB006592, 2010

Mechanics of active magmatic intraplating in the Rio Grande Rift near Socorro, New Mexico

J. Pearse[1] and Y. Fialko[1]

Received 5 May 2009; revised 3 February 2010; accepted 8 March 2010; published 20 July 2010.

[1] We investigate long-term deformation due to the Socorro Magma Body (SMB), one of the largest active intrusions in the Earth's continental crust, using interferometric synthetic aperture radar (InSAR) observations and finite element simulations. InSAR data spanning 15 years (1992–2007) indicate that the magma body is associated with a steady crustal uplift at a rate of about 2 mm yr^{-1}. Previous work showed that while the pattern of surface uplift is consistent with an elastic inflation of a large sill-like magma body, the SMB could not have formed via steady elastic inflation because the latter would be outpaced by magma solidification. We resolve this problem using coupled thermo-visco-elastic models, and place constraints on the intrusion history as well as the rheology of the ambient crustal rocks. We demonstrate that observations rule out the linear Maxwell response of the ductile crust, but are consistent with laboratory-derived power law rheologies. Our preferred model suggests that the age of the SMB is of the order of 10^3 years, and that the apparent constancy of the present-day uplift may be due to slow heat transfer and ductile deformation in a metamorphic aureole of a giant sill-like magma intrusion, rather than due to a steady increase in the magma overpressure. The SMB is a contemporaneous example of "magmatic intraplating," a process by which large volumes of mafic melt stall and spread at midcrustal depths due to density or rheology contrasts.

Citation: Pearse, J., and Y. Fialko (2010), Mechanics of active magmatic intraplating in the Rio Grande Rift near Socorro, New Mexico, *J. Geophys. Res.*, *115*, B07413, doi:10.1029/2009JB006592.

1. Introduction

[2] Magmatic processes play a fundamental role in the formation and chemical differentiation of the Earth's crust. Observations of a high velocity layer at the base of the continental crust [*Mooney and Brocher*, 1987] and high seismic reflectivity of the lower crust [*Fuchs*, 1969; *Brown et al.*, 1987; *de Voogd et al.*, 1988] suggest that considerable volumes of mantle-derived melts were added to the base of the crust through a process termed "magmatic underplating" [*Furlong and Fountain*, 1986; *Bergantz*, 1989]. Intrusion of mantle-derived melts into the lower crust results in advection of heat and partial melting of the less refractory host rocks, which (along with other processes, such as differentiation of mantle melts) produces much of the granulite residue and silica-enriched melts that eventually form the upper continental crust [*Huppert and Sparks*, 1988; *Bohlen and Mezger*, 1989; *Sisson et al.*, 2005; *Annen et al.*, 2006]. The mechanisms and dynamics of magma ponding in the lower crust (in particular, characteristic deformation rates and timescales), as well as the shape and size of individual intrusions are poorly known. In this paper we discuss long-term geodetic measurements of deformation due to one of the largest and deepest known magma intrusions in the Earth's continental crust, the Socorro Magma Body (SMB) in New Mexico. Previous studies suggested that the SMB is associated with surface uplift occurring at a constant rate of a few millimeters per year [*Reilinger and Oliver*, 1976; *Larsen et al.*, 1986; *Fialko and Simons*, 2001; *Finnegan and Pritchard*, 2009]. We interpret the available geodetic data using coupled thermomechanical models of the magma body's evolution to resolve the "thermomechanical paradox" of the SMB [*Fialko and Simons*, 2001], which arises because the expected thermal lifetime of the sill is much less than the thousands of years required for it to grow by steady elastic inflation. We begin with a suite of mechanical models, in which we use geodetic constraints such as the shape and rate of surface uplift and physical considerations such as the range of admissible magma overpressures to estimate the age of the intrusion and constrain the rheology of the crust. We then consider thermophysical models to address the thermomechanical paradox, and assess the importance of thermal effects such as stress relaxation and thermal expansion of melting host rock on the reservoir overpressures. We also discuss implications for the emplacement of giant midcrustal magma bodies and physics of magmatic accretion in the continental crust.

2. Analysis of Geodetic Data

[3] The Socorro Magma Body (SMB) is located in the middle of the Rio Grande Rift in central New Mexico (see

[1]Institute of Geophysics and Planetary Physics, Scripps Institution of Oceanography, University of California, San Diego, La Jolla, California, USA.

0148-0227/10/2009JB006592

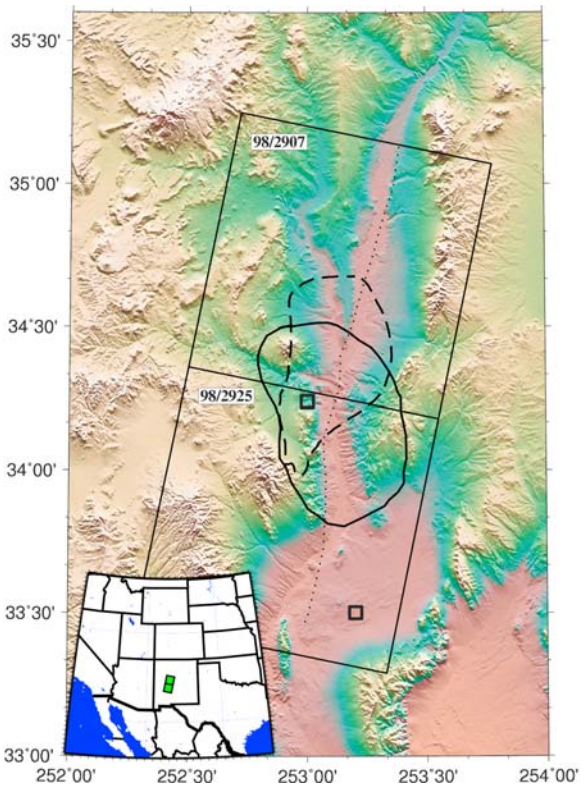

Figure 1. Topography map of the Socorro, New Mexico, region showing the ERS track and frames used in this study. The solid line [*Balch et al.*, 1997] and dashed line [*Rinehart and Sanford*, 1981] denote the extent of seismic reflector determined by seismic studies. The dotted line is the leveling route from *Larsen et al.* [1986] study. The open black squares near the center of the SMB and to the south denote areas used for the time series analysis of LOS (see Figure 4).

Figure 1). Although there is currently no active volcanism in the region, the latter experienced substantial magmatic activity since the onset of rifting during the Tertiary [e.g., *McMillan et al.* 2000]. Upwelling of the asthenosphere has been inferred from teleseismic studies in the rift [*Parker et al.*, 1984]. Upwelling of hot mantle material is presumably responsible for the anomalously high heat flow at the surface [*Reiter*, 2005], and magma supply to the crust. At Socorro, seismic studies have discovered an unusually strong reflector with horizontal dimensions of 50–70 km, at a depth of about 19 km [*Sanford et al.*, 1973]. High impedance contrasts and strong conversion phases associated with the midcrustal reflector have been interpreted as requiring the presence of fluid, most likely melt, in the middle crust beneath Socorro [*Rinehart and Sanford*, 1981; *Balch et al.*, 1997]. The estimated thickness of the melt layer is of the order of several tens of meters, based on modeling of observed micro-earthquake reflections [*Ake and Sanford*, 1988]. *Ake and Sanford* [1988] argued that there is a second layer of slightly higher velocity and roughly the same thickness below the melt layer, which they attributed to an earlier partially solidified intrusion. The Earth's crust in the vicinity of the reflector is characterized by high seismicity (the Socorro Seismic Anomaly covers ~2% of the area of the state of New Mexico but accounts for ~45% of its seismicity above magnitude 2.5 [*Balch et al.*, 1997]), anomalously high electrical conductivity [*Hermance and Neumann*, 1991], and a long-term uplift. Leveling surveys conducted between 1911 and 1981 estimated average uplift rates of a few millimeters per year [*Larsen et al.*, 1986]. A subsequent study using a limited set of interferometric synthetic aperture radar (InSAR) collected by the ERS-1 and 2 satellites data over a time interval of 7 years between 1992 and 1999 mapped the surface extent of the uplift and showed that deformation associated with the magma body is still ongoing and that the uplift persists at a rate of 2–3 mm yr^{-1} [*Fialko and Simons*, 2001]. The apparent constancy of surface uplift due to the SMB is remarkable, given that other neovolcanic areas are characterized by episodic unrest on timescales of months to years [*Langbein et al.*, 1995; *Dvorak and Dzurisin*, 1997; *Chang et al.*, 2007], presumably reflecting variations in magma supply from a deep source. Note that the large depth of the inferred magma body, as well as large wavelength and temporal persistence of the observed surface deformation at Socorro suggest that the latter is unlikely to be caused by hydrothermal activity. To establish whether the crustal uplift above the SMB indeed continues at a steady rate, and whether there is any variability in the uplift rate on shorter timescales (e.g., months to years), we requested the European Space Agency to resume radar acquisitions in the Socorro area in 2005. Although the ERS-2 satellite suffered a loss of gyroscopes in year 2000, some acquisitions made in the zero gyro mode since 2005 have radar Doppler values that allow interferometric pairing with earlier data. To quantify the time dependence of surface deformation in the Socorro area, we processed the whole catalog of European Remote-Sensing Satellites ERS-1 and 2 data from the descending satellite track 98. The catalog data consists of several tens of radar acquisitions collected over a time period of 15 years between 1992 and 2007 (Figure 2). We used these data to generate a set of 95 radar interferograms. The data were processed using JPL/Caltech software suite ROI_PAC and a 1 arc second digital elevation model from the Shuttle Radar Topography Mission [*Farr and Kobrick*, 2000]. We investigated a possible variability in the uplift rates on timescales less than 5 years using subsets of interferograms covering different epochs [*Fialko*, 2006]. Figure 3 shows the average line of sight (LOS) velocities from 1992–1996, 1996–2000, and 2000–2007 observation epochs derived from stacking of the respective interferograms (Figure 2). Interferometric pairs used for stacking were optimally selected to minimize contribution of scenes most affected by the atmospheric noise [*Rivet and Fialko*, 2007]. LOS velocities toward the satellite are taken to be positive. Dome-like uplift at a rate of 2–3 mm yr^{-1} can be clearly seen in each of these stacks in the region corresponding approximately with the intersection of the two seismically inferred outlines of the crustal reflector. The data shown in Figure 3 indicate that the inflation of the SMB has occurred at an essentially constant rate over the last 15 years. Note there is also a broad area of subsidence to the south, which may be a result of magma withdrawal from a deeper source, as discussed in section 4. In addition to stacking subsets of interferograms from different epochs, we performed a time series analysis [*Berardino et al.*, 2002; *Schmidt and Bürgmann*, 2003] to investigate possible changes in the uplift rate on timescales less than 5 years. For every coherent

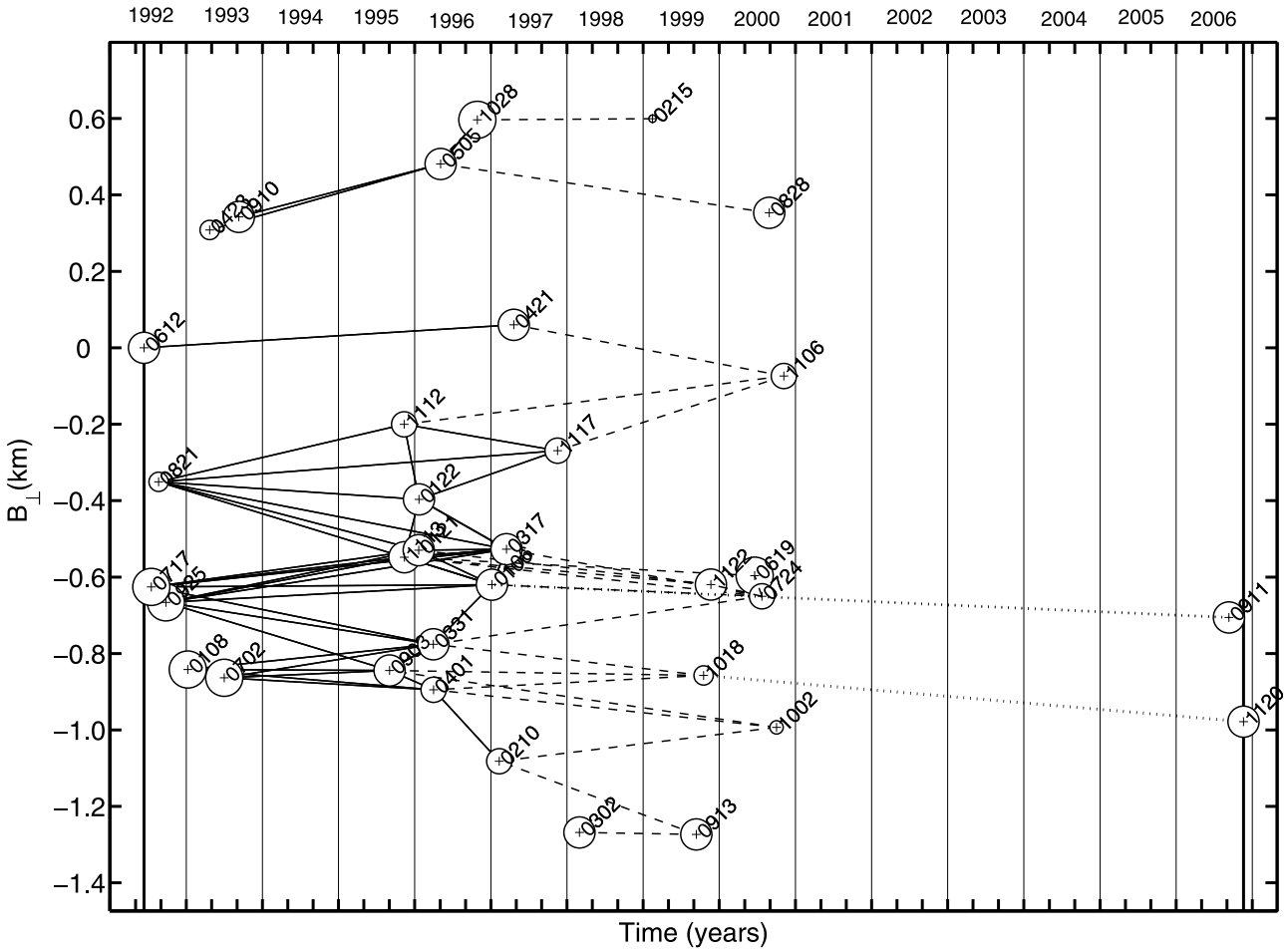

Figure 2. ERS-1 and -2 radar data from track 98 used in stacking. Circles denote radar acquisitions; the size of the circles is proportional to the estimated atmospheric noise in each scene [*Rivet and Fialko*, 2007]. Numerical labels denote orbit numbers. Horizontal axis represents time, and vertical axis represents a perpendicular baseline (separation between repeat orbits). Solid lines denote interferometric pairs covering 1992–1996 epoch (see Figure 3a), dashed lines denote pairs covering 1996–2000 epoch (see Figure 3b), and dotted lines denote pairs covering 2000–2006 epoch (see Figure 3c).

interferogram in our data set, we calculated range changes between a ~30 km^2 area centered on the SMB uplift, and a reference area to the south (see Figure 1). The obtained range changes (along with the respective time intervals) were assembled into a linear system of equations, which was solved for the time history of LOS displacements using singular value decomposition. The resulting time history is shown in Figure 4 (squares). As one can see from Figure 4, the inferred rate of deformation appears to be constant within the uncertainty of our measurements. We obtain a non-biased estimate of the uplift rate, using a least squares linear fit to the time series [e.g., *Jacobs et al.*, 2002; *Fialko*, 2004] as shown in Figure 4 by a solid line. The corresponding LOS velocities are 2–2.2 mm yr^{-1}, in good agreement with average velocities inferred from stacking (Figure 3) and results of *Finnegan and Pritchard* [2009].

[4] A comparison of the InSAR measurements with the historic leveling data further suggests that the inflation persisted at a steady rate over the last 100 years. Figure 5 shows the average uplift rate as a function of distance along a north-south leveling profile (see Figure 1) over a time period 1912–1951 (adapted from *Larsen et al.* [1986]), as well as the average LOS velocities derived from the most recent (2000–2007) InSAR data along the same profile. As one can see from Figure 5, both the wavelength and the magnitude of uplift due to the SMB are quite consistent between the different data sets and observation periods.

3. Modeling of the Emplacement History of the Socorro Magma Body

[5] Elastic models of sill-like magma bodies indicate that intrusions with characteristic horizontal dimensions in excess of the emplacement depth should produce a surface uplift comparable to the intrusion thickness [*Fialko et al.*, 2001a]. Assuming that the inflation rate has been constant since the inception of the SMB, the geodetically measured uplift rate of 2–3 mm yr^{-1} and the seismically inferred thickness of the SMB of several tens of meters [*Ake and Sanford*, 1988] suggest the age of the magma body of the order of 10^4–10^5 years [*Larsen et al.*, 1986]. However, steady elastic inflation of the SMB is not thermally viable

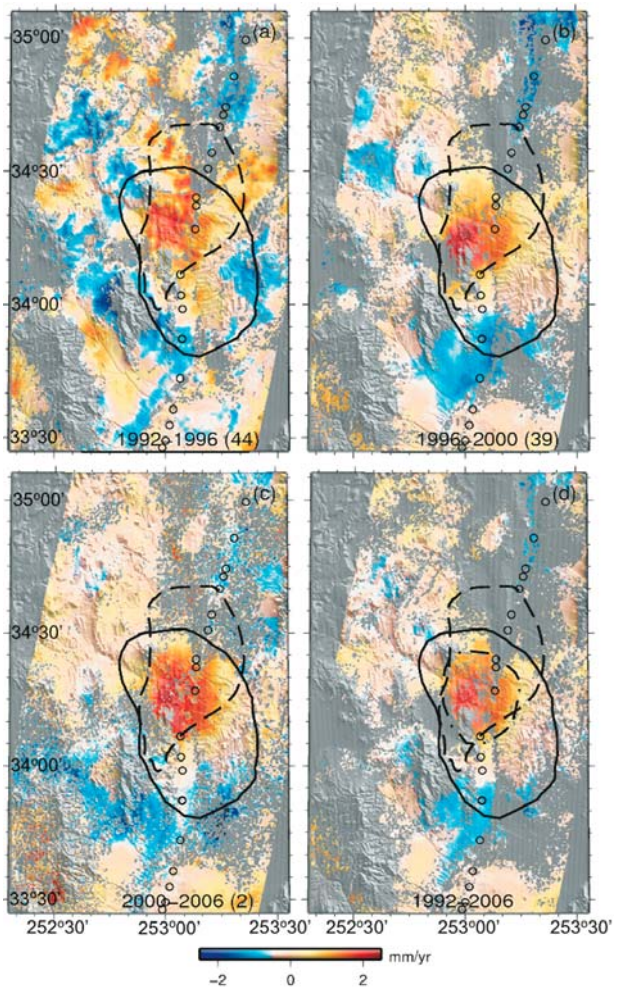

Figure 3. Average line of sight (LOS) velocities from 4 stacks of interferograms spanning a 15 year time period from early 1992 to late 2006. Positive velocities indicate motion toward the satellite. Numbers in parentheses denote number of interferograms used for stacking (a) 1992–1996; (b) 1996–2000; (c) 2000–2006; (d) is the average of the velocity fields shown in Figures 3a–3c. The solid outline [*Balch et al.*, 1997] and dashed outline [*Rinehart and Sanford*, 1981] denote the seismically imaged reflector. The north-south trending circles show the from the level-line benchmark locations from the *Larsen et al.* [1986] study. The dot-dashed line in Figure 3d is the outline of the magma body used in our numerical models.

over thousands of years, since the solidification rate of the injected magma would significantly out-pace the elastic opening rate [*Fialko and Simons*, 2001; *Fialko et al.*, 2001b]. Solidification of a sill due to conductive heat loss to the ambient rocks occurs at an average rate of the order of κ/w, where w is the intrusion thickness and κ is the thermal diffusivity of the host rock [*Carslaw and Jaeger*, 1959]. Assuming a total uplift of the order of the current thickness of the magma body ($\sim 10^2$ m) [*Ake and Sanford*, 1988] and $\kappa = 10^{-6}$ m^2/s, the solidification rate is of the order of a few tens of centimeters per year. Thus, the geodetically determined rate of sill opening in case of elastic deformation is at least an order of magnitude smaller than the estimated solidification rate, which constitutes the "thermomechanical paradox" of the SMB. Available geomorphologic data suggest that uplift could not have exceeded 100 m since the Pliocene [*Bachman and Mehnert*, 1978], and may be less than 50 m [*Finnegan and Pritchard*, 2009]. This suggests that the total volume of magma injected in the SMB could not significantly exceed the present-day volume inferred from seismic studies [*Ake and Sanford*, 1988], unless the intrusion was accommodated by predominantly inelastic mechanisms. Substantial inelastic deformation is implied by the fact that the strain associated with the emplacement of SMB given by the ratio of the characteristic thickness (tens of meters) to the characteristic in-plane dimension (tens of kilometers) is of the order of 10^{-3}, well above the elastic limit for rocks (10^{-5}–10^{-4}). Similarly, the excess pressure required to produce the observed thickness greatly exceeds the rock tensile strength (~10 MPa), even if one neglects the stress concentration at the intrusion tips. At the same time, the inference of a predominantly inelastic accommodation of the SMB needs to be reconciled with the fact that the geodetically measured uplift over the last 10^2 years is well explained by models assuming a purely elastic inflation of a source which location and size is consistent with seismic observations: inelastic deformation around a source of the same size would likely produce a broader surface uplift pattern [*Fialko and Simons*, 2001; *Fialko et al.*, 2001b].

[6] To resolve the thermodynamic and mechanical problems associated with the emplacement of the SMB we performed a series of numerical experiments that take into account plausible deformation mechanisms and heat transfer associated with intrusion of large crustal sills into the lower crust. We consider a range of emplacement histories. All simulations begin with intrusion of a large magma sheet having initial magma overpressure of up to 10 MPa, after which overpressure is either constant, or changes with time at a constant rate between ±5 kPa yr^{-1}. Note that these bracketing values of increasing/decreasing pressure rates were chosen as extreme end-member cases, and would be expected to give much larger surface uplift rates than are seen

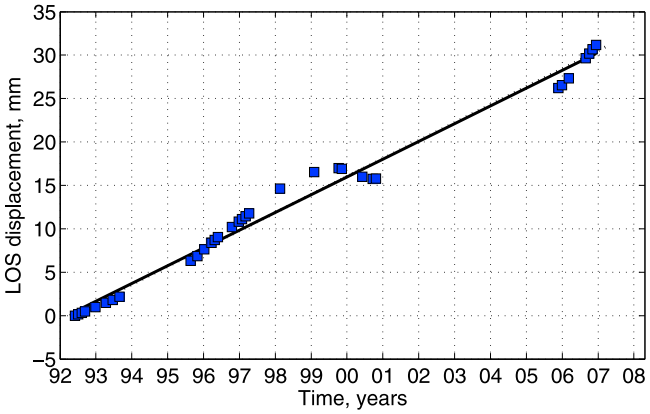

Figure 4. Time series of LOS displacements due to the Socorro Magma Body. Squares denote LOS displacements of the central part of the uplift with respect to a stable area south of Socorro (see Figure 1). Solid line represents the least squares linear fit to the data treating time and LOS displacements as independent variables [*Fialko*, 2004].

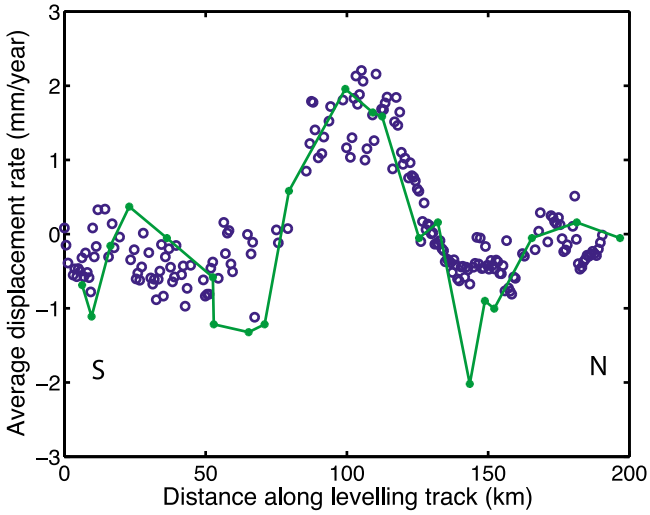

Figure 5. A comparison of uplift rate inferred from leveling data from 1912 to 1951, projected onto the InSAR LOS vector (solid line [*Larsen et al.*, 1986]) and LOS velocity inferred from InSAR data (hollow circles) from the 2000–2006 stack (see Figure 3c), along the leveling route (see Figures 1 and 3).

in the data (in the case of increasing pressure) or subsidence (in the case of decreasing pressure). Purely elastic models, in which all the surface deformation is generated by steadily increasing pressure on the reservoir walls (without accounting for viscoelastic relaxation in the midcrust), require a pressure increase rate of approximately 0.6 kPa yr^{-1} to fit the uplift data [*Fialko et al.*, 2001b]. Therefore we would expect, in our viscoelastic models, that the rates of pressure increase as high or higher than this value would greatly overpredict surface uplift rates. This is confirmed by the results of our numerical experiments which show that when viscoelastic relaxation is included, pressure increase/decrease rates could not exceed 0.5 kPa yr^{-1} (section 3.1).

[7] We seek models that satisfy the following physical and observational constraints: (1) magma overpressure (i.e., the difference between magma pressure and lithostatic stress) cannot exceed the rock tensile strength. The pressure boundary condition is applied at the walls of the reservoir. (2) The rate of mechanical opening of the magma reservoir walls due to magma overpressure must out-pace the rate of solidification. (3) The rate and shape of the concomitant crustal uplift over the last 100 years must be consistent with geodetic data. The goal of these experiments is to determine a physically reasonable pressure history within the SMB, estimate the age of the intrusion, and constrain the rheology of the host rocks.

[8] Time- and temperature-dependent simulations of deformation due to intrusion of a large sill-like magma body were performed using the finite element code ABAQUS. We assumed a depth of emplacement of 19 km based on seismic data [*Sanford et al.*, 1973; *Ake and Sanford*, 1988; *Balch et al.*, 1997]. The initial geometry of the magma body was inferred by fitting the InSAR data with boundary element models assuming elastic deformation and an excess pressure that increases with time at a constant rate. The inferred sill geometry (see dotted outline in Figure 3d) was then used to generate a finite element mesh (see Figure 6). The mesh represents a cube with an edge length of 300 km. The sides and bottom of the mesh are prescribed zero-displacement boundary conditions, and the top is stress-free. The uppermost 12-km thick layer is taken to be elastic, based on the depth distribution of earthquake hypocenters [*Rinehart and Sanford*, 1981; *Stankova et al.*, 2008]. Because the SMB is located in the middle crust, well below the brittle-ductile transition, it is reasonable to assume that the intrusion of magma is accompanied by a significant ductile flow of the host rocks. The ductile response of the ambient crust is likely enhanced by elevated geotherms below the Rio Grande Rift, as well as by the advected specific and latent heat of magma. Our simulations tested a variety of rheologies for material below the brittle-ductile transition, including linear Maxwell and power law rheologies. A constitutive relationship for a viscoelastic material is given by the following expression [*Kirby and Kronenberg*, 1987; *Ranalli*, 1995]:

$$\dot{\epsilon} = A\sigma^n e^{(-Q/RT)} + \frac{\dot{\sigma}}{E} \tag{1}$$

where $\dot{\epsilon}$ is the strain rate (units of s^{-1}), A is the power law coefficient ($Pa^{-n}\ s^{-1}$), σ is the deviatoric stress (Pa), n is the power law exponent, Q is the activation energy (J mol^{-1}), R is the universal gas constant (J $mol^{-1}\ K^{-1}$), T is the temperature (K) and E is the Young's modulus (Pa). Effective viscosity of a power law material can be expressed as

$$\eta = \sigma^{(1-n)} e^{(Q/RT)}/2A \tag{2}$$

For the special case of a Maxwell material ($n = 1$), effective viscosity is $e^{(Q/RT)}/2A$. Initial simulations were performed for the simplified case of temperature-independent power law rheology of the form $\dot{\epsilon} = C\sigma^n + \frac{\dot{\sigma}}{E}$ to constrain the power law exponent and the pre-multiplying coefficient C. Here, C is a constant that replaces $A\ e^{(-Q/RT)}$ in equation (1). In these models, the middle and lower crust are treated as a uniform material with rheological properties which are independent of composition or temperature. Our estimates of C therefore provide an approximate "average" value of $Ae^{(-Q/RT)}$ for the bulk of the lower crust.

[9] In the first set of temperature-independent models we apply a constant overpressure of 10 MPa within the reservoir, and examine the rate and pattern of uplift for the Maxwell rheologies ($n = 1$) with viscosities varying from 10^{17} to 10^{19} Pa s, power law rheologies with n varying from 2.5 to 3.5, and C varying from 10^{-14} to 10^{-16} MPa^{-n}. Geodetic data indicate that the SMB did not expand laterally over the last 100 years (Figure 5). All simulations assume a Young's modulus of the host rocks of 20 GPa (lower than the seismically inferred values, to account for a likely frequency dependence of the elastic moduli of the crust).

3.1. Results of Mechanical Modeling

[10] Predicted surface displacements are highly sensitive to the model rheology. Figure 7a shows the time histories of uplift rate for five trial rheologies: two Maxwell models with viscosities of 10^{18} Pa s and 10^{19} Pa s and three power law models with power law exponents of 3.5 and power law

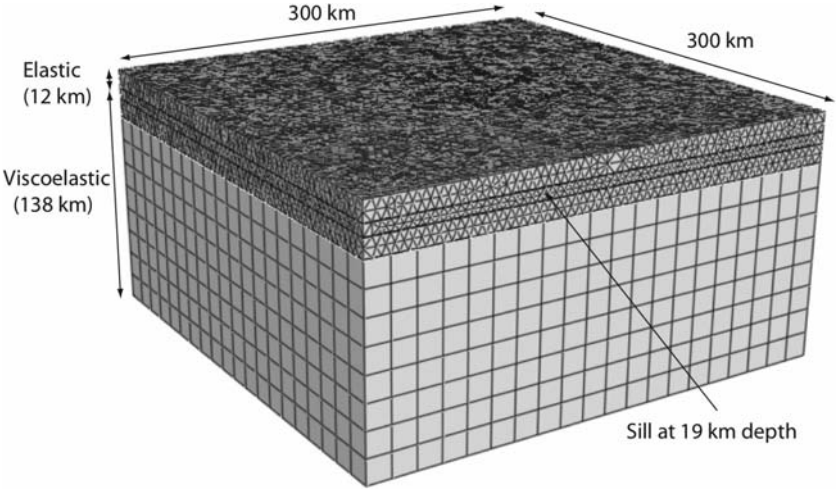

Figure 6. A mesh cube showing the finite element model setup in ABAQUS. The cube is 300 km by 300 km, with a total depth of 150 km. The uppermost 12 km is purely elastic, and the lower 138 km is viscoelastic. The sill, not visible, is embedded inside the cube at a depth of 19 km.

multipliers of 10^{-14} MPa^{-n}, 10^{-15} MPa^{-n} and 10^{-16} MPa^{-n} (corresponding to effective viscosities of 10^{17} Pa s, 10^{18} Pa s and 10^{19} Pa s respectively, for a deviatoric stress of 10 MPa).

[11] The initial elastic uplift of approximately 8 m at the onset of emplacement is followed by a fairly rapid viscoelastic response. Note that purely elastic models require that the surface uplift rate and the rate of volume increase of the magma reservoir be directly proportional to the rate of increase of magma overpressure within the reservoir; thus if we apply an instantaneous pressure of 10 MPa at the beginning of the simulation and keep it constant thereafter, the elastic solution for surface displacement would show an initial jump to 8 m and remain at that value, and surface uplift rates would be zero.

[12] The viscoelastic models entail a more complex relationship between the rates of uplift, overpressure and magma supply. In particular, viscoelastic models predict surface uplift even if magma overpressure is maintained at a constant value, as relaxation of deviatoric stresses in the host rock induces additional deformation in the rest of the crust, as well as gives rise to a continued increase in the volume of the magma reservoir. Both the rate of uplift and the rate of increase of the reservoir's thickness (and thus the rate of volume increase) decay with time according to the viscoelastic relaxation time. Figure 8 shows the rate of increase of the thickness of the sill at its center, for four of the example rheologies tested in our mechanical models. Figure 8a shows the total uplift at the surface, and Figure 8b shows the thickness of the reservoir at its center. We point out that in these temperature-independent calculations melting in the host rock is not considered, so increases in the reservoir volume imply influx of new magma. In contrast with the elastic case (for which surface uplift rates are equal to rates of increase in the sill thickness), viscoelastic deformation allows the sill thickness to increase at a much higher rate compared to the surface uplift. Enhanced opening of the sill helps offset the effects of solidification. Given a constant overpressure, the uplift rate due to viscoelastic relaxation decays over time, at a rate which depends on the ductile properties of the host rocks. The age of the initial emplacement therefore has a strong control on the calculated uplift histories.

[13] All of the tested models produce surface uplift rates of 2–3 mm yr^{-1} at some point within 3500 years of the initiation of emplacement. In general, lower effective viscosities of the host rocks lead to the observed uplift rates sooner, and create reservoirs that open faster; however, they also result in surface uplifts that are much broader than the observed one. Figure 7b shows the uplift rate along a profile through the center of the uplift for three of the test rheologies, taken at times when the peak uplift rate is approximately 2.5 mm yr^{-1}: the Maxwell model with viscosity 10^{19} Pa s, and the power law models with exponent 3.5 and power law coefficients of 10^{-15} and 10^{-16} MPa^{-n}. The broadening of the surface uplift is most sensitive to the power law exponent, with lower powers producing a much worse fit to the data for a given effective viscosity. In particular, the Maxwell rheologies create much broader patterns of surface uplift compared to the observed one, even on timescales of 100 years or less. This misfit cannot be circumvented just by using higher viscosities: increasing the viscosity causes the reservoir to open more slowly, effectively reducing the solution to the elastic one. Thus there is a trade-off between keeping the surface uplift narrow enough, and allowing the reservoir to open fast enough to avoid solidification. None of the Maxwell models can resolve this trade-off. Models using Maxwell rheology might be reconciled with the geodetic data if one assumes a smaller initial size of the SMB, such that the broadening of the uplift over time may produce the present uplift pattern. However, as seen in Figure 7b, the broadening of the uplift pattern for the Maxwell rheology is significant over the time required to bring the surface uplift to its current rates (almost a factor of 3), and thus an intrusion with substantially smaller horizontal dimensions would be required in order for the model results to match the current uplift rates. This is problematic for a number of reasons. First of all, a much smaller sill would not be consistent with the seismically inferred boundaries of the crustal reflector. In addition, solidification rates are higher for a smaller reservoir, so its thermal lifetime would be reduced. Finally, smaller reservoirs

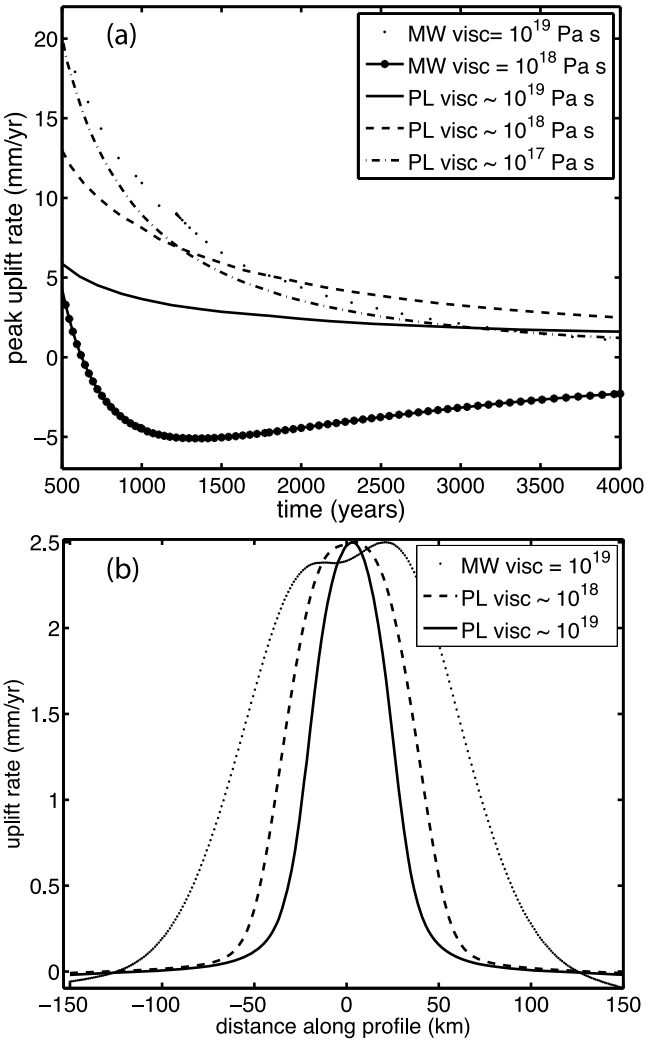

Figure 7. (a) Comparison of peak uplift rates as a function of time for five models: Maxwell rheologies with viscosities of 10^{18} Pa s and 10^{19} Pa s, and power law rheologies with power law exponents of 3.5, and with effective viscosities of 10^{17} Pa s, 10^{18} Pa s and 10^{19} Pa s for a deviatoric stress of 10 MPa. (b) Uplift rate along a profile through the center of the model surface displacement for three rheologies, taken at times when the peak uplift rate is ~2.5 mm yr^{-1}: a Maxwell model with viscosity 10^{19} Pa s (at t = 2600 years), and power law models with power law exponent 3.5 and effective viscosities of 10^{18} Pa s (at t = 4000 years) and 10^{19} Pa s (at t = 1900 years). Note that the Maxwell models produce a characteristic eventual "sagging" of the velocity profile above the center of the intrusion.

would require unrealistically high initial overpressures to achieve the observed uplift rates. A slight asymmetry in the predicted displacement in case of the Maxwell model (see Figure 7b) is due to the asymmetry of the source (a benchmark simulation with an axially symmetric penny-shaped crack produces an axisymmetric displacement pattern).

[14] The trade-off between the uplift shape and the reservoir thickness is fortuitous in that it considerably narrows the range of candidate rheologies. We find that the observational constraints are best met by using a power law relationship with exponent $n = 3.5$, and multipliers of the order of 10^{-16} MPa^{-n} s^{-1} (corresponding to an effective viscosity of the order of 10^{19} Pa s at deviatoric stresses of 10 MPa). Viscosities an order of magnitude higher lead to intrusions that open too slowly to avoid solidification, and viscosities an order of magnitude lower lead to surface uplift patterns that broaden too quickly. For our best fit rheology, the surface uplift reaches a rate of 3 mm yr^{-1} at about 1400 years after emplacement, and decays to 2 mm yr^{-1} by about 2500 years after emplacement. The total reservoir thickness at $t = 1400$ years is approximately 60 m (yielding an average opening rate of 4.3 cm yr^{-1}), and at $t = 2500$ years the reservoir thickness is about 75 m (average opening rate of 3 cm yr^{-1}). However, by $t = 1700$ years, the uplift pattern is becoming too broad. Thus the time of

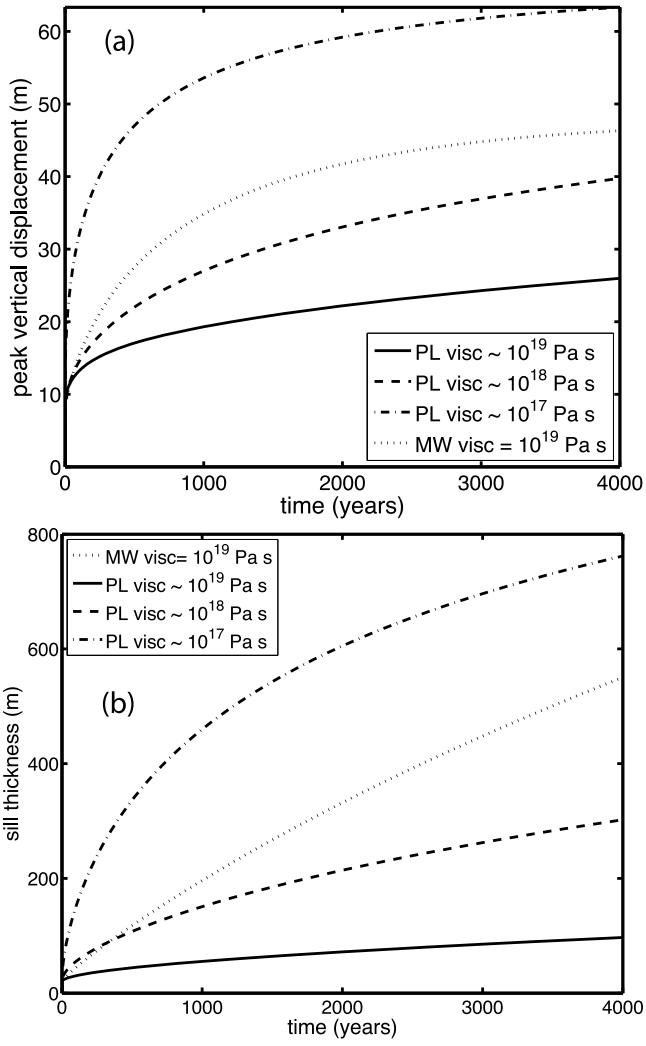

Figure 8. (a) Peak uplift at the surface as a function of time for four mechanical models: A Maxwell rheology with viscosity 10^{19} Pa s, and power law rheologies with power law exponents of 3.5, and with effective viscosities of 10^{17} Pa s, 10^{18} Pa s and 10^{19} Pa s for a deviatoric stress of 10 MPa. (b) Thickness of the sill (measured at the center of the sill's cross section) as a function of time for the same four mechanical models.

emplacement based on this model is estimated between about 1400 and 1600 years ago, with the best fit at about 1500 years after the emplacement. The average reservoir opening rate is of the same order of magnitude as the average solidification rate, with the most rapid opening occurring in the early stages, thereby allowing the reservoir to evolve to its present state without intermittent solidification.

[15] Numerical experiments with variable pressure histories indicate that the initial excess pressure may be lowered somewhat if the pressure is allowed to increase with time. Physically, this can be interpreted as injecting a smaller amount of magma during the initial pulse, but then adding magma at a rate that is larger than the injection rate required to keep the overpressure constant during viscoelastic relaxation. In our experiments we tried initial overpressures as low as 5 MPa, but found that there was a minimum starting overpressure below which pressure increase rates greater than 0.5 kPa yr^{-1} would be required to explain the current thickness of the magma body; such pressure rates, however, tend to overpredict the current uplift rates [*Fialko et al.*, 2001b]. Models with higher initial overpressures lead to the most rapid early opening of the reservoir, and are more likely to be thermally viable, as well as more consistent with the seismically inferred thickness of the reservoir. Decreases in the excess pressure since the emplacement (e.g., due to crystallization, degassing, or melt loss via satellite intrusions) produce uplift rates that decay more rapidly with time. However, we found that if magma pressure is decreased by more than about 0.5 kPa yr^{-1}, then the uplift rate is predicted to change noticeably within the 100 year interval when the average uplift rate is of the order of millimeters per year, contrary to the geodetic constraint of a steady uplift. Our calculations bracket the initial overpressures between 8 MPa and 10 MPa, rate of pressure change between ± 0.5 kPa yr^{-1}, and the time of emplacement between 900 and 1600 years ago.

3.2. Effects of Heat Flow and Temperature-Dependent Rheology

[16] Results from temperature-independent models allow us to narrow down the plausible range of power law parameters and intrusion ages that satisfy thermodynamic and geodetic constraints on the history of the SMB, however they ignore the effects of heat transfer on the rheology of the host rocks adjacent to the magma body. To investigate such effects we used fully coupled thermomechanical models accounting for the conductive heat loss from the SMB and the temperature-dependent viscosity of the ambient crust. We adopt the best fitting temperature-independent rheology and explicitly include the Arrhenius factor $e^{(Q/RT)}$, with Q = 260 kJ mol^{-1} K^{-1} [*Kirby and Kronenberg*, 1987]. Temperature-dependent calculations assume the initial host rock temperature of 870 K, and magma temperature of 1520 K. We tested a range of the initial host rock temperatures and found that the model predictions are not very sensitive to the assumed initial temperature, as long as the viscoelastic relaxation times of the heated host rock are small compared to the age of the intrusion. The latter condition is met for the rock temperature in excess of 900 K, and the age of the intrusion in excess of $10–10^2$ years. The exponential temperature dependence of the Arrhenius factor leads to a sharp transition from material whose characteristic relaxation time is many orders of magnitude below the inferred timescale of the intrusion (i.e., 10^3 years) to material which can maintain some stresses over that time period (in this case, our best fitting rheology, whose decay curves can be seen in Figure 7a). Thus there is effectively a boundary of undetectable thickness, over which the viscosity changes from the "cold" rheology, to material with viscosities so low that it would not be able to support any appreciable deviatoric stress on the timescale of geodetic observations ($1–10^2$ years).

[17] Conductive heat loss from the magma reservoir results in enhanced relaxation of deviatoric stress in the adjacent ductile crust and increased uplift rates. This is because the expanding halo of hot low-viscosity material surrounding the reservoir is mechanically equivalent to an increase in the effective size of the reservoir for a given magma overpressure [*Dragoni and Magnanensi*, 1989; *Newman et al.*, 2006]. Viscous relaxation is most pronounced at the periphery of the intrusion, resulting in a significant blunting of the tips and reduction in the stress concentration. This relaxation may effectively limit lateral propagation of magma sills, as well as prevent climbing of sills with large diameter-to-depth ratios toward the Earth's surface expected in case of the elastic-brittle response of the host rocks [*Fialko*, 2001].

[18] Ductile flow of the host rocks may also considerably alter the shape of the reservoir. Figure 9 shows a comparison of the reservoir shapes for elastic and thermally activated power law rheologies. Elastic models predict that for intrusions with the characteristic horizontal dimension in excess of the intrusion depth, most of the reservoir opening is accommodated by uplift of the roof [*Fialko et al.*, 2001a]. In contrast, large sill intrusions in the ductile middle and lower crust may have a nearly uniform thickness and grow predominantly by depression of the bottom of the sill, due to a buttressing effect of the elastic upper crust. In this case, the total amplitude of surface uplift may be much smaller than the average thickness of the intruded sill.

[19] We note that the enhanced relaxation due to temperature-dependent rheology is confined to a conductive boundary layer around the intrusion, and does not substantially affect the wavelength of the surface uplift compared to temperature-independent models at a given time after the onset of intrusion. Thus our choice of power law parameters, which was constrained by the broadening of the uplift pattern, is not altered by adding in the temperature dependence. The latter, however, allows one to reduce the initial overpressure, as the uplift rates for a given applied overpressure are larger due to the the expanding halo of low-viscosity material. Based on a number of simulations, we find that initial pressures that are lower than 7 MPa create reservoirs that are thinner than suggested by seismic data, at the time when the surface deformation fits the geodetic data. Initial pressures higher than 7 MPa increase the age of the emplacement so that the surface deformation pattern becomes too broad at the time when the predicted uplift rate matches the observed one. Using an initial overpressure of 8 MPa, for instance, the observed uplift rate is reached at approximately 2300 years after the onset of intrusion, but by that time the uplift pattern is already much too broad to fit the InSAR data. Figure 10 shows a comparison between the InSAR data and predictions of our best fitting temperature-dependent model assuming the age of the SMB of 1430 years,

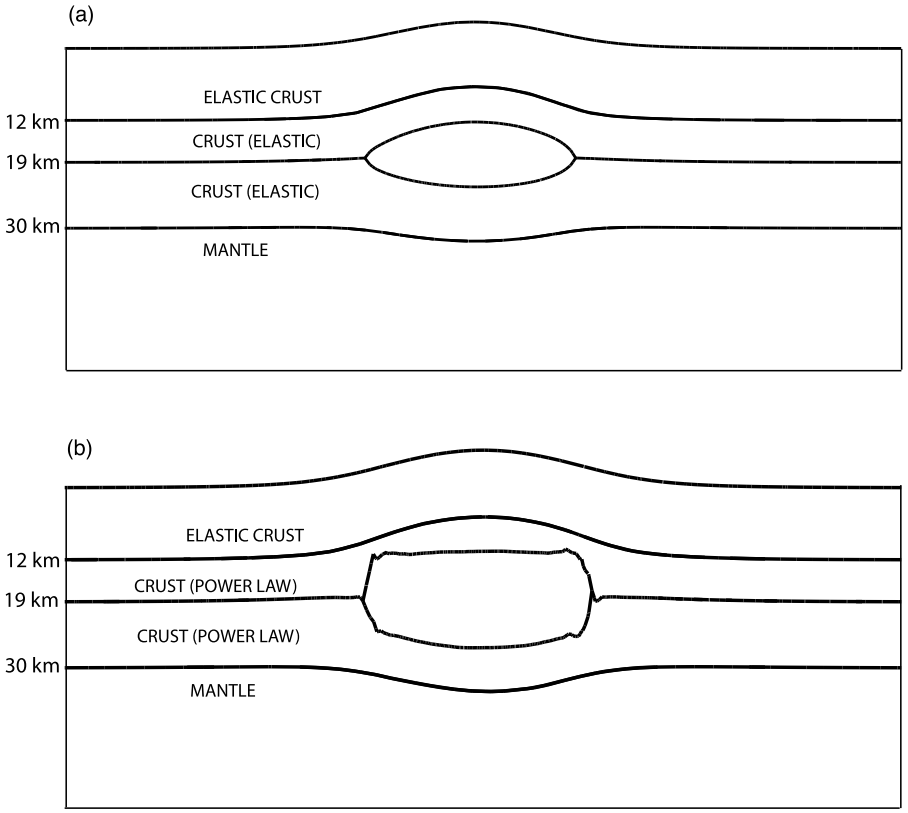

Figure 9. Cross sections of a sill-like magma body predicted by numerical models assuming different rheologies. (a) Purely elastic crust and mantle. (b) Best fitting viscoelastic model with temperature-dependent power law rheology. Vertical scale is greatly exaggerated.

and the excess magma pressure of 7 MPa. The predicted reservoir thickness at $t = 1430$ years is about 42 m, implying an average opening rate of about 3 cm yr^{-1}.

[20] These coupled thermomechanical calculations did not explicitly include phase transitions or thermal expansion. Thermal expansion of the host rock may also generate uplift (and thus contribute to the total effective overpressure assumed in our mechanical models), although the expansion of the host rock is partially offset by the contraction of the cooling magma. A more significant effect would be expected from density changes associated with phase changes: when hot basaltic magma is injected into the crust, melting of the host rock (which presumably generates magma of a more silicic composition) occurs as the basalt solidifies [*Huppert and Sparks*, 1988; *Annen and Sparks*, 2002]. Again, effects of the expansion associated with melting of the host rock would be at least partly offset by contraction of the solidifying basalt. However, since the crustal rock and basaltic intrusion likely have different solidi and latent heat of fusion (approximately 550 kJ/kg for basalt versus ~350 KJ/kg for crustal rocks), the volume of host rock melt is expected to exceed the volume of the solidifying basaltic intrusion, and some host rock melt may remain even after the intruded basalt has completely frozen. Fully coupled mechanical and thermal simulations quantifying the relative contributions of magma injection rate, thermal expansion and phase changes to the total uplift are beyond the scope of this paper. Instead, in section 3.3 we present a thermodynamic model that lends support to inferences from our viscoelastic simulations. In particular, we will show that the scenario represented by our best fitting mechanical model is, in fact, consistent with the present-day existence of melt, for a plausible range of assumptions about the thermal history of the region. Based on the results of these experiments, we will also argue that the seismic reflection anomaly beneath Socorro most likely represents melted host rock rather than basalt from the original magma intrusion. Finally we will demonstrate that expansion associated with melting of the host rocks can produce overpressures of the same order of magnitude as those estimated from our mechanical modeling, so that this mechanism alone can sustain the uplift, without requiring any further addition of basalt.

3.3. Thermal Viability of the SMB

[21] Our best fitting viscoelastic model (ignoring thermal effects) assumed a constant overpressure of 10 MPa, and a power law rheology with a power law exponent of 3.5 and an effective viscosity of 10^{19} Pa s for deviatoric stresses of 10 MPa. This model generates uplift of 2.5 mm yr^{-1} and an approximately 70 m thick magma body 1400 years after the initial emplacement (see Figure 8b). In the presence of solidification, such thickness is not large enough to explain the seismologic inference of a contemporaneous melt layer with thickness of the order of tens of meters. In fact, a

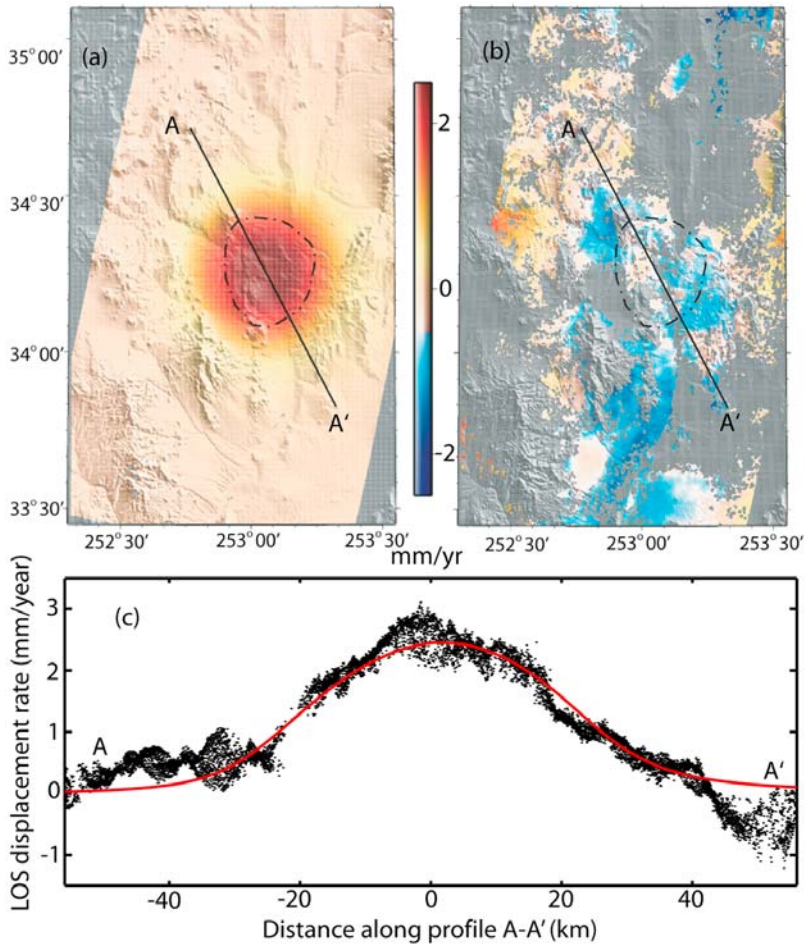

Figure 10. Comparison of the best fitting SMB model with the InSAR data. (a) The predicted LOS velocity 1430 years after the onset of intrusion. (b) The residual InSAR data after subtracting the modeled LOS velocity. (c) The LOS velocity along the profile A-A′ for the model (red solid line) and the InSAR data (black dots).

reservoir with a fixed thickness of 70 m is expected to completely solidify on a timescale of approximately 100 years. Here we explore a possibility that the seismic reflector represents the residual silicic magma generated by melting of the host rocks. First, we model the instantaneous emplacement of a 70 m thick basaltic sheet. Simulations are performed using the finite element software ABAQUS. The initial temperature within the reservoir is set at 1520 K, and the initial host rock temperature is assumed to be 870 K (corresponding to the geothermal gradient of 30 K/km [*Reiter*, 2005]). The simulations allow phase changes within both the reservoir and the host rock. We use a latent heat of fusion of 550 kJ/kg for the basalt and 350 KJ/kg for the host rock. The solidus temperature of the basalt is assumed to be 1270 K and the solidus temperature of the host rock is assumed to be 1120 K. Simulations indicate that the basaltic sill solidifies within 100 years; while the host rock melt is initially produced, it also solidifies in less than 250 years if no more magma is injected. Figure 11 shows the temperature profile from the center of the basaltic sill to a distance of 300 m, at 93 years after the initial intrusion (solid line in Figure 11). Abscissa represents distance (in meters) from the center of the intrusion; the basalt layer ends at x = 35 m. There is no remaining melt above the solidus temperature of basalt (1270 K), so the initial intrusion is frozen. However, there is a significant amount of host rock that is above the solidus temperature of 1120 K. Dashed line in Figure 11 shows the same profile at 230 years after the intrusion: by this time, there is no remaining host rock melt. We conclude that under these conditions, our best fitting mechanical model would not be expected to retain any seismically detectable melt after 1400 years. As discussed in section 3.2, decreases in the viscosity that allow for larger reservoirs also lead to misfit with the observed shape of the surface uplift, and increases in the initial thickness results in unrealistic overpressures. We note that large effective overpressure may in principle be used to simulate the effect of multiple intrusions that tightly cluster in space and time. However, we found that a 20 MPa overpressure at least doubles the time required to achieve uplift rates of 2–3 mm yr^{-1}. Allowing viscoelastic relaxation to continue for this long leads to a large misfit with the shape of the surface uplift, even for viscosities as high as 10^{19} Pa s. Pressure could be steadily decreased from the original value of 20 MPa to force the desired uplift rates at 1400 years (which occurs if pressure is

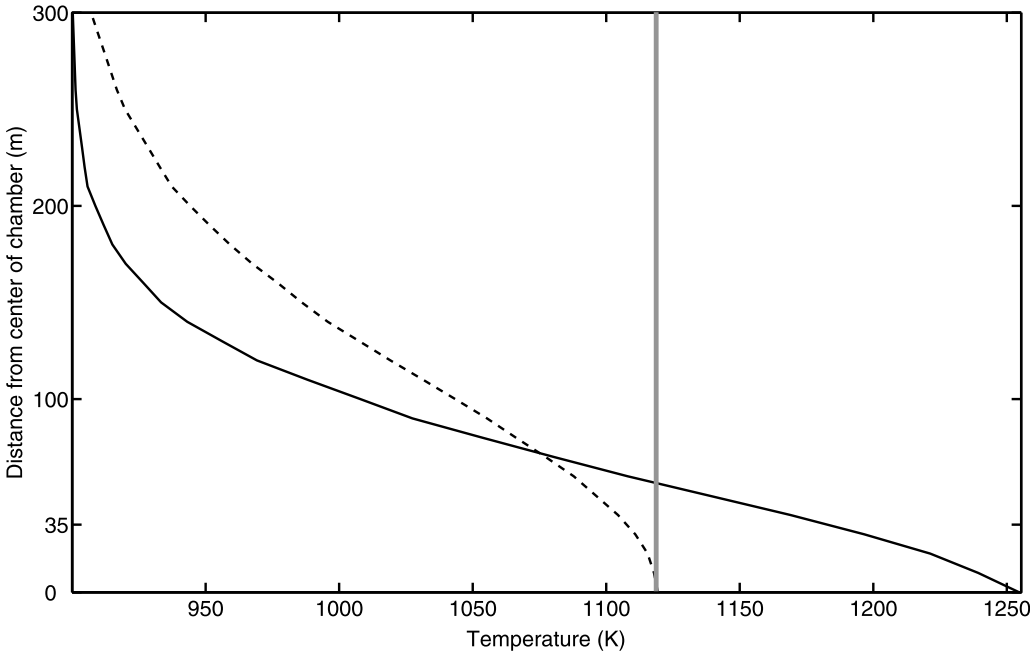

Figure 11. Temperature profiles for a 70 m intrusion into cold crust: 93 years after the intrusion (solid line) and 230 years after the intrusion (dashed line). Distance along the y axis represents the vertical distance from the center of the intrusion. The edge of the basalt layer is at y = 35 m. At 93 years, all the material within the basalt layer is below the basalt solidus of 1270 K; however, within the host rock layer (y >35 m) some material is still above the host rock solidus of 1120 K (represented by the vertical grey line). At 230 years, all of the basalt and host rock is solidified.

lowered at a rate of approximately 3 kPa yr^{-1}), but even then, the uplift pattern still does not fit the data.

[22] Another variable affecting the thermal lifetime of the intrusion is the ambient temperature. It is recognized that extensional tectonics and/or previous magma intrusions may substantially raise the host rock temperature and produce long-lived thermal anomalies. Such anomalies may allow episodic basaltic intrusions as thin as 50 m to produce large volumes of crustal melt [*Annen and Sparks*, 2002]. To explore the effect of potential deviation of temperature in the middle crust beneath Socorro from the normal geothermal gradient, we introduce a local temperature anomaly at depth of the SMB, as shown in Figure 12. This anomaly is introduced by "preheating" the crust with two intrusions 1000 years apart and is used as an initial condition for the best fitting mechanical model. We point out that the assumed elevated temperature of the crust at the emplacement level of the SMB admit multiple explanations, and the profile shown in Figure 12 is merely an example. We find that following the emplacement of a 70-m thick basaltic sill into the preheated host rock, some basaltic melt remains for up to 340 years, and large volumes of silicic melt are produced (Figure 13, solid line). At 1400 years after the intrusion (Figure 13, dashed line) a significant amount of host rock melt remains (at least 100 m on each side of the intrusion). These simulations lend support to the hypothesis that the long-term geodetic uplift and seismic inferences of a thin melt layer are most consistent with melting of the host rocks due to intrusion of mantle magma into a preheated middle crust beneath Socorro.

[23] As noted above, expansion of the melting host rock may be an additional source of overpressure which drives uplift. As long as some basaltic melt remains, the pressure drop associated with contraction of the solidifying basalt will offset the pressure increase associated with expansion of the melting host rock. In these early stages, the overpressure within the reservoir is most likely maintained predominantly by continued influx of new magma. Once the basalt solidifies completely, the remaining host rock melt may continue to exert overpressure. The amount of overpressure supplied by the remaining layer of melt is $\Delta p \sim \Delta V/(V\beta)$, where $\Delta V/V$ is the fractional change in volume that accompanies melting and β is the compressibility of the melt. Assuming a fractional volume increase of ~1% on melting, and a melt compressibility of 10^{-9} Pa^{-1}, this gives an overpressure of approximately 10 MPa. Therefore even if the supply of new basaltic magma is cut off and no basaltic melt remains, the host rock melt may maintain an overpressure of approximately the same magnitude that we used in our mechanical models. These examples illustrate that despite its relatively short thermal life time, a 70 m basaltic magma reservoir may have a sufficient thermal inertia, both from increase in the effective size of the reservoir due to relaxation of stresses in the expanding halo of low-viscosity material surrounding the reservoir, as well as from volume changes associated with melting of the host rock. These can be viewed as effective contributors to the overpressure prescribed in our mechanical models. Even if injection of new magma is stopped after a few hundred years, the rapid initial emplacement of a large volume of magma can generate the observed uplift on timescale of 10^3 years.

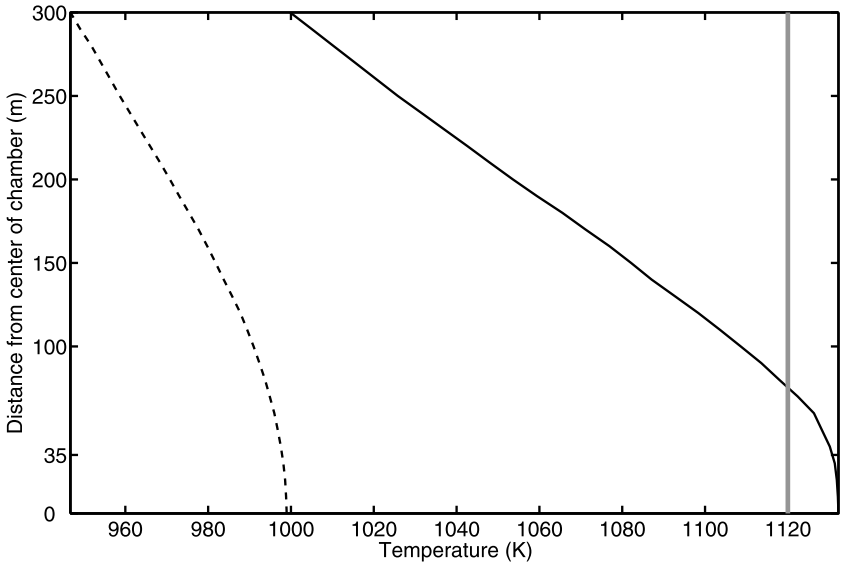

Figure 12. The temperature profile resulting from two repeated (superimposed) 70 m intrusions, occurring 1000 years apart. The solid profile shows temperature as a function of vertical distance from the center of the intrusion, 1000 years after the second intrusion. This profile was used as an initial condition for our simulation of the thermal evolution of the SMB. The dashed line shows the temperature profile 1000 years after the first intrusion, but before the second, for comparison. The initial condition, before any intrusions, was T = 1520 K inside the intrusion, and T = 900 K outside. The vertical grey line shows the host rock solidus.

[24] We point out that this 70 m per 1000 year intrusion rate is an example designed to illustrate how effective repeated intrusions can be in prolonging the thermal lifetime of an individual intrusion, but presumably in the case of SMB, a much lower frequency of intrusion would suffice. However, as demonstrated by *Annen and Sparks* [2002], rates of repeated intrusion less than about 50 m per 100,000 years are too low for large-scale melt generation. This in particular

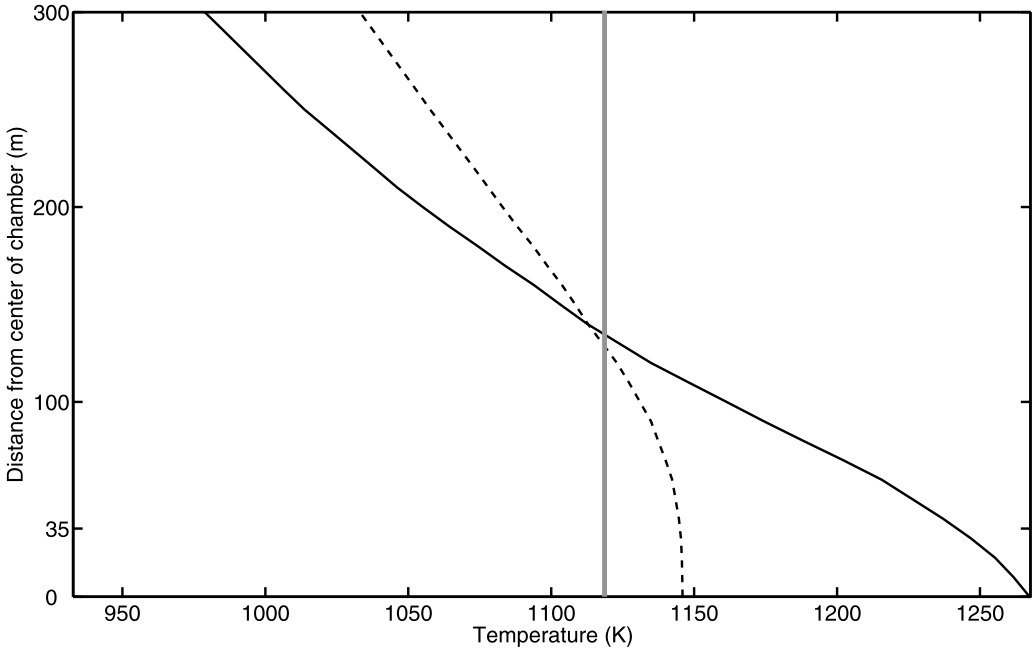

Figure 13. Temperature profiles for a 70 m intrusion into crust given initial conditions shown in Figure 11. The solid line gives the temperature profile at 340 years after the intrusion. All of the basalt layer is below the solidus temperature (1270 K). However, a large volume of host rock remains above the crustal solidus (1120 K, represented by the vertical grey line). The dashed line shows the temperature profile for the same intrusion, 1400 years after its emplacement. Although no basaltic melt remains, close to 100 m of the host rock remains above the solidus.

reinforces our claim that there is no way to produce a present-day melt layer, especially not a melt layer of thickness on the order of tens of meters, by slow steady injection of magma on timescales greater than 10^4 years.

4. Discussion and Conclusions

[25] Using numerical modeling (including both mechanical and thermal considerations) constrained by geodetic data, we have presented a scenario for the development of the Socorro Magma body which (1) explains the shape and rates of uplift seen in the geodetic data, (2) is consistent with seismic estimates of the location and depth of the chamber and (3) is thermally viable based on plausible thermal histories of the region - and thus resolves the thermomechanical paradox.

[26] Results of our numerical experiments suggest that the unusually constant uplift around Socorro may not be indicative of a steady magma injection, but may instead represent ductile relaxation of the lower crust and large thermal inertia of the SMB. This interpretation does not preclude a continued supply of new melt into the SMB over its history (e.g., as observed in other neovolcanic areas). The respective magma flux decays with time and cannot significantly exceed the calculated rate of viscoelastic increase in the SMB volume.

[27] From the mechanical modeling, we conclude that the steady uplift rate can be well-explained by a rapid intrusion followed by viscoelastic deformation, without appealing to a slowly inflating sill in an elastic crust (which we reject on the grounds that the required rate of growth of the sill would be outpaced by orders of magnitude by the rate of solidification of the intrusion). Our suggestion that the intrusion must have begun as a rapid emplacement of a sizable magma sheet is based on the fact that very slow, gradual opening would be impeded by rapid solidification (even in the presence of a localized thermal anomaly), which means that the intrusion needs a reasonable "head start" in order to preserve melt on timescales of the order of 10^2–10^3 years. In addition, the amount of overpressure exerted on the chamber walls in that initial pulse must be substantial (of order of megapascals), because exerting a significantly smaller amount of overpressure in the initial intrusion would reduce the subsequent viscoelastic opening rate of the chamber.

[28] The available data also allow us to make robust inferences about the effective rheology of the Earth's crust below the brittle-ductile transition within the Rio Grande Rift. In particular, our mechanical models rule out linear Maxwell rheology of the middle and lower crust. Our inference of a power law midcrustal rheology at Socorro follows from geodetic constraints of the surface uplift patterns, and is independent of any assumptions about heat flow, or about what specific contributions are being made to the pressure within the sill. The best fitting power law rheology with thermally activated creep is consistent with laboratory data [*Kirby and Kronenberg*, 1987] as well as the transient response of the lower crust and upper mantle following large earthquakes [*Freed and Bürgmann*, 2004] and deglaciation [*Wu*, 2001; *Gasperini et al.*, 2004].

[29] Based on results of our simulations of heat transfer associated with the emplacement of the SMB, we argue that the magma overpressure is unlikely to be sustained only by continual intrusion of new basalt. Results of the thermodynamic analysis confirm our conclusions from the mechanical modeling, demonstrating that (1) our mechanical model estimates of rapid emplacement of a magma sheet, followed by viscoelastic uplift on timescales of thousands of years, is consistent with what would be thermally viable in a volcanic region such as Socorro, within the range of plausible thermal histories of the region; and (2) our estimates of the magnitude of the overpressure, based on the outcome of mechanical modeling, are consistent with a combination of basalt intrusion, expansion associated with host rock melting, and relaxation of stresses in a hot halo surrounding the chamber.

[30] Geodetic and seismic observations of the SMB are instructive for understanding the dynamics and timescales of events involved in magmatic accretion of the Earth's continental crust. Emplacement of large mafic sills is believed to play a key role in the crustal genesis [*Huppert and Sparks*, 1988; *Laube and Springer*, 1998; *Petford et al.*, 2000], however the timescales and rates of individual intrusions remain poorly constrained despite numerous geochemical, petrological and geophysical studies [*Hawkesworth et al.*, 2004]. Theoretical arguments suggest that the emplacement of large crustal sills in extended terrains should preferentially occur at the crust-mantle boundary [*Parsons et al.*, 1992]. This is because deviatoric stresses supported by the lower crust may be small compared to deviatoric stresses in the uppermost mantle, so that dikes that arrive from the mantle may switch the direction of the minimum compressive stress above the Moho from horizontal to vertical if the excess magma pressure overwhelms the deviatoric stress in the crust, thereby encouraging subsequent magma emplacement in sills. At the same time, all giant magma bodies discovered in the Earth's continental crust by seismic studies, including the SMB, the Altiplano-Puna magma body (South America) [*Chmielowski et al.*, 1999; *Yuan et al.*, 2000] and the Tibet magma body [*Nelson et al.*, 1996; *Brown et al.*, 1996] are located at depths of about 20 km, and are best characterized as magmatic "intraplates" rather than "underplates". Ubiquitous seismic "bright spots" that presumably manifest active or crystallized magma sills also commonly reside at depths between 15 to 20 km, i.e., well above the Moho [*Lachenbruch et al.*, 1985; *de Voogd et al.*, 1988; *Jarchow et al.*, 1993]. These observations, along with recent geological and petrological inferences of prevalent magmatic accretion at mid-crustal depths [*Barboza and Bergantz*, 2000; *Yoshino and Okudaira*, 2004] lend support to the idea that the ascending mantle melts may be trapped at various levels within the continental crust. It so, both the lower and middle crust may be involved in anatexis and generation of silicic magmas. The mechanisms for trapping of large volumes of mantle melts may be different. Rheological contrasts such as the one proposed at the Moho might be responsible for underplating [*Parsons et al.*, 1992], although the long-term strength of the lower crust versus upper mantle is a matter of debate [e.g., *Jackson*, 2002; *Pollitz et al.*, 2001; *Fialko*, 2004; *Barbot et al.*, 2008]. However, the mechanism considered by *Parsons et al.* [1992] is not applicable in the middle crust, unless the ductile strength of the crust increases with depth. Therefore the depth of magmatic intraplating must be controlled by other mechanisms - for example, the so-called level of neutral buoyancy for mantle-derived melts [*Bradley*, 1965; *Herzberg*

et al., 1983; *Ryan et al.*, 1983; *Lister and Kerr*, 1991; *Ryan*, 1993, 1994]. We point out that the level of neutral buoyancy may be a necessary but not a sufficient condition for emplacement of sills in the middle crust. Dikes that transport magma from a deep source will have little tendency to turn into sills at the level of neutral buoyancy if the least compressive stress remains horizontal at that level, as expected in areas of extensional tectonics such as the Rio Grande Rift. Instead, dike intrusions will spread laterally in the direction of the intermediate principal stress and (eventually) solidify, reducing the differential stress in the crust. If magma influx overwhelms tectonic extension, the least compressive stress will first reach a lithostatic value at the level of neutral buoyancy because the excess magma pressure is greatest at that level [e.g., *Fialko and Rubin*, 1998]. Subsequent magma supply in dikes will further increase the horizontal stress, and sill intrusions may be initiated. For this reason exposures of early, transcrustal dike swarms along old continental rift zones [*Cather*, 1990; *Mohr*, 1992] do not preclude the possibility that the emplacement of sill intrusions at midcrustal levels is controlled by the density contrasts between the magma and the host rocks. The Socorro Magma Body is a vivid example of an ongoing emplacement of a large midcrustal sill in an active continental rift. The observed rates of extension in the Rio Grande Rift are low [*Savage et al.*, 1985], implying that switching of the principal stresses in the crust may be accomplished with relatively minor magmatic input.

[31] The geodetically measured steady state uplift rate due to the Socorro Magma Body of a few millimeters per year is intriguingly similar to the average growth rates of large crustal plutons deduced from geochronologic studies [*Coleman et al.*, 2004; *Hawkesworth et al.*, 2004; *Matzel et al.*, 2006], which suggests similar governing mechanisms, regardless of differences in tectonic environments. As discussed in section 2, the historic uplift rate (Figure 5) underestimates the average growth rate of the SMB, perhaps by as much as an order of magnitude, because the historic uplift doesn't account for the initial sill intrusion, and because the intrusion is accommodated primarily by the floor depression (rather than by roof uplift). At the same time, it is recognized that the emplacement of large plutons may be highly non-steady and involve multiple episodes of sill intrusions [*Coleman et al.*, 2004; *Glazner et al.*, 2004; *Matzel et al.*, 2006; *Annen et al.*, 2006]. Taking our inferred emplacement history of the SMB at face value, the average rate of sill opening of ~50 mm yr^{-1} (70 m over 1400 years) and the magma flux of order of 3–5 × 10^{-2} km^3 yr^{-1} (corresponding to the effective sill radius of ~15 km) may be consistent with the geochronologically estimated rates of the pluton growth if the average "recurrence" interval of the magmatically robust episodes is of the order of 10^4 years.

[32] A "bottom-down" growth of the SMB predicted by our models (see Figure 9) is able to explain a modest (if any) total uplift at the Earth's surface suggested by geomorphologic data [*Bachman and Mehnert*, 1978; *Finnegan and Pritchard*, 2009] and is consistent with geologic observations of exhumed plutons [*Paterson and Fowler*, 1993; *Cruden*, 1998; *Grocott et al.*, 1999]. We point out that our simulations do not include withdrawal of melt from a presumed mantle source, and are applicable even in the case of a deep or laterally distributed source. If the source region feeding the SMB is shallow (e.g., lies above the Moho) one may expect a "piston" or "cantilever"-type subsidence of the lower-crustal block between the inflating SMB and the deflating magma source [e.g., *Cruden*, 1998]. Such a deformation mechanism might manifest itself via subsidence at the periphery of uplift due to the SMB [*Fialko and Simons*, 2001]. Steady subsidence to the south of the SMB apparent in the InSAR data (see Figure 3) might be related to magma withdrawal from a deep source and a complex ductile response of the lower crust to the emplacement of the SMB, although additional studies are required to explore such a possibility.

[33] Taken together, thermodynamic, geodetic, and seismic constraints provide useful insights into the timing and vigor of the latest intrusion event associated with the SMB. Observations appear to be best explained by a rapid emplacement of a large magma sill into preheated crust about 10^3 years ago, followed by melting of the host rocks due to their lower solidus compared to the mantle-derived magma (presumably of mafic composition). Note that once an intrusion and the surrounding melted host rock have both solidified completely, there is no excess pressure to drive further uplift. As shown by our thermodynamic experiments as well as previous studies [e.g., *Annen and Sparks*, 2002], injected melts solidify rather quickly, whereas the thermal anomalies produced by them last considerably longer. Thus it is likely that previous (if any) intrusions at Socorro had solidified by the time the latest event was initiated, while still leaving behind a thermal anomaly that allowed the most recent intrusion to continue to drive the present-day uplift.

[34] **Acknowledgments.** We acknowledge thoughtful comments from Roland Burgmann, an anonymous reviewer and the Associate Editor Michael Ryan. This work was supported by NSF (grants EAR-0450035 and 0944336). Original SAR data are copyright of the European Space Agency, acquired via the WInSAR Consortium at UNAVCO. We thank Wolfgang Lengert for including the Rio Grande Rift area in the background mission of the ERS-2 satellite in 2005–2007.

References

Ake, J. P., and A. R. Sanford (1988), New evidence for the existence and internal structure of a thin layer of magma at mid-crustal depths near Socorro, New Mexico, *Bull. Seismol. Soc. Am.*, *78*, 1335–1359.

Annen, C., and R. S. J. Sparks (2002), Effects of repetitive emplacement of basaltic intrusions on thermal evolution and melt generation in the crust, *Earth Planet. Sci. Lett.*, *203*, 937–955, doi:10.1016/S0012-821X(02)00929-9.

Annen, C., J. D. Blundy, and R. S. J. Sparks (2006), The genesis of intermediate and silicic magmas in deep crustal hot zones, *J. Petrol.*, *47*, 505–539, doi:10.1093/petrology/egi084.

Bachman, G. O., and H. H. Mehnert (1978), New K-Ar dates and the late Pliocene to Holocene geomorphic history of the central Rio Grande region, New Mexico, *Geol. Soc. Am. Bull.*, *89*, 283–292, doi:10.1130/0016-7606(1978)89<283:NKDATL>2.0.CO;2.

Balch, R. S., H. E. Hartse, A. R. Sanford, and K. Lin (1997), A new map of the geographic extent of the Socorro magma body, *Bull. Seismol. Soc. Am.*, *87*, 174–182.

Barbot, S., Y. Hamiel, and Y. Fialko (2008), Space geodetic investigation of the coseismic and postseismic deformation due to the 2003 M_w 7.1 Altai earthquake: Implications for the local lithospheric rheology, *J. Geophys. Res.*, *113*, B03403, doi:10.1029/2007JB005063.

Barboza, S., and G. Bergantz (2000), Metamorphism and anatexis in the mafic complex contact aureole, Ivrea zone, northern Italy, *J. Petrol.*, *41*, 1307–1327, doi:10.1093/petrology/41.8.1307.

Berardino, P., G. Fornaro, R. Lanari, and E. Sansosti (2002), A new algorithm for surface deformation monitoring based on small baseline differential SAR interferograms, *IEEE Trans. Geosci. Remote Sens.*, *40*, 2375–2383, doi:10.1109/TGRS.2002.803792.

Bergantz, G. W. (1989), Underplating and partial melting: Implications for melt generation and extraction, *Science*, *245*, 1093–1095, doi:10.1126/science.245.4922.1093.

Bohlen, S. R., and K. Mezger (1989), Origin of granulite terranes and the formation of the lowermost continental crust, *Science*, *244*, 326–329, doi:10.1126/science.244.4902.326.

Bradley, J. (1965), Intrusion of major dolerite sills, *Trans. R. Soc. N. Z.*, *3*, 27–55.

Brown, L. D., et al. (1987), COCORP: New perspectives on the deep crust, *Geophys. J. R. Astron. Soc.*, *89*, 47–54.

Brown, L. D., et al. (1996), Bright spots, structure, and magmatism in Southern Tibet from INDEPTH seismic reflection profiling, *Science*, *274*, 1688–1690, doi:10.1126/science.274.5293.1688.

Carslaw, H. S., and J. C. Jaeger (1959), *Conduction of Heat in Solids*, 2nd ed., 243 pp., Oxford Univ. Press, London.

Cather, S. M. (1990), Stress and volcanism in the northern Mogollon-Datil volcanic field, New Mexico: Effects of the post-Laramide tectonic transition, *Geol. Soc. Am. Bull.*, *102*, 1447–1458, doi:10.1130/0016-7606(1990)102<1447:SAVITN>2.3.CO;2.

Chang, W.-L., R. B. Smith, C. Wicks, J. M. Farrell, and C. M. Puskas (2007), Accelerated uplift and magmatic intrusion of the Yellowstone Caldera, 2004 to 2006, *Science*, *318*, 952–956, doi:10.1126/science.1146842.

Chmielowski, J., G. Zandt, and C. Haberland (1999), The central Andean Altiplano-Puna magma body, *Geophys. Res. Lett.*, *26*, 783–786, doi:10.1029/1999GL900078.

Coleman, D. S., W. Gray, and A. F. Glazner (2004), Rethinking the emplacement and evolution of zoned plutons: Geochronologic evidence for incremental assembly of the Tuolumne Intrusive Suite, *Calif. Geol.*, *32*, 433–436.

Cruden, A. R. (1998), On the emplacement of tabular granites, *J. Geol. Soc.*, *155*, 853–862, doi:10.1144/gsjgs.155.5.0853.

de Voogd, B., L. Spera, and L. Brown (1988), Crustal extension and magmatic processes: COCORP profiles from the Death Valley and the Rio Grande Rift, *Geol. Soc. Am. Bull.*, *100*, 1550–1567, doi:10.1130/0016-7606(1988)100<1550:CEAMPC>2.3.CO;2.

Dragoni, M., and C. Magnanensi (1989), Displacement and stress produced by a pressurized, spherical magma chamber, surrounded by a viscoelastic shell, *Phys. Earth Planet. Inter.*, *56*, 316–328, doi:10.1016/0031-9201(89)90166-0.

Dvorak, J., and D. Dzurisin (1997), Volcano geodesy: The search for magma reservoirs and the formation of eruptive vents, *Rev. Geophys.*, *35*, 343–384, doi:10.1029/97RG00070.

Farr, T., and M. Kobrick (2000), Shuttle Radar Topography Mission produces a wealth of data, *Eos Trans. AGU*, *81*, 583.

Fialko, Y. (2001), On origin of near-axis volcanism and faulting at fast spreading mid-ocean ridges, *Earth Planet. Sci. Lett.*, *190*, 31–39, doi:10.1016/S0012-821X(01)00376-4.

Fialko, Y. (2004), Evidence of fluid-filled upper crust from observations of postseismic deformation due to the 1992 M_w7.3 Landers earthquake, *J. Geophys. Res.*, *109*, B08401, doi:10.1029/2004JB002985.

Fialko, Y. (2006), Interseismic strain accumulation and the earthquake potential on the southern San Andreas fault system, *Nature*, *441*, 968–971, doi:10.1038/nature04797.

Fialko, Y., and M. Simons (2001), Evidence for on-going inflation of the Socorro magma body, New Mexico, from Interferometric synthetic aperture radar imaging, *Geophys. Res. Lett.*, *28*, 3549–3552, doi:10.1029/2001GL013318.

Fialko, Y., Y. Khazan, and M. Simons (2001a), Deformation due to a pressurized horizontal circular crack in an elastic half-space, with applications to volcano geodesy, *Geophys. J. Int.*, *146*, 181–190, doi:10.1046/j.1365-246X.2001.00452.x.

Fialko, Y., M. Simons, and Y. Khazan (2001b), Finite source modeling of magmatic unrest in Socorro, New Mexico, and Long Valley, California, *Geophys. J. Int.*, *146*, 191–200, doi:10.1046/j.1365-246X.2001.00453.x.

Fialko, Y. A., and A. M. Rubin (1998), Thermodynamics of lateral dike propagation: Implications for crustal accretion at slow-spreading mid-ocean ridges, *J. Geophys. Res.*, *103*, 2501–2514, doi:10.1029/97JB03105.

Finnegan, N. J., and M. E. Pritchard (2009), Magnitude and duration of uplift above the Socorro magma body, *Geology*, *37*, 231–234, doi:10.1130/G25132A.1.

Freed, A. M., and R. Bürgmann (2004), Evidence of power-law flow in the Mojave desert mantle, *Nature*, *430*, 548–551, doi:10.1038/nature02784.

Fuchs, K. (1969), On the properties of deep crustal reflectors, *J. Geophys.*, *35*, 133–149.

Furlong, K. P., and D. M. Fountain (1986), Continental crustal underplating: Thermal considerations and seismic-petrologic consequences, *J. Geophys. Res.*, *91*, 8285–8294, doi:10.1029/JB091iB08p08285.

Gasperini, P., G. Dal Forno, and E. Boschi (2004), Linear or non-linear rheology in the Earth's mantle: the prevalence of power-law creep in the postglacial isostatic readjustment of Laurentia, *Geophys. J. Int.*, *157*, 1297–1302, doi:10.1111/j.1365-246X.2004.02319.x.

Glazner, A. F., J. M. Bartley, D. S. Coleman, W. Gray, and R. Taylor (2004), Are plutons assembled over millions of years by amalgamation from small magma chambers?, *GSA Today*, *14*, 4–11, doi:10.1130/1052-5173(2004)014<0004:APAOMO>2.0.CO;2.

Grocott, J., A. Garde, B. Chadwick, A. Cruden, and C. Swager (1999), Emplacement of rapakivi granite and syenite by floor depression and roof uplift in the Palaeoproterozoic Ketilidian orogen, south Greenland, *J. Geol. Soc.*, *156*, 15–24, doi:10.1144/gsjgs.156.1.0015.

Hawkesworth, C., R. George, S. Turner, and G. Zellmer (2004), Time scales of magmatic processes, *Earth Planet. Sci. Lett.*, *218*, 1–16, doi:10.1016/S0012-821X(03)00634-4.

Hermance, J. F., and G. A. Neumann (1991), The Rio Grande Rift: New electromagnetic constraints on the Socorro magma body, *Phys. Earth Planet. Sci.*, *66*, 101–117, doi:10.1016/0031-9201(91)90107-S.

Herzberg, C. T., W. F. Fyfe, and M. J. Carr (1983), Density constraints on the formation of the continental Moho and crust, *Contrib. Mineral. Petrol.*, *84*, 1–5, doi:10.1007/BF01132324.

Huppert, H. E., and R. S. J. Sparks (1988), The generation of granitic magmas by intrusion of basalt into continental crust, *J. Petrol.*, *29*, 599–624.

Jackson, J. (2002), Strength of the continental lithosphere: Time to abandon the jelly sandwich?, *GSA Today*, *12*, 4–9, doi:10.1130/1052-5173(2002)012<0004:SOTCLT>2.0.CO;2.

Jacobs, A., D. Sandwell, Y. Fialko, and L. Sichoix, and the The 1999 (2002), (M_w7.1) Hector Mine, California, earthquake: Near-field postseismic deformation from ERS interferometry, *Bull. Seismol. Soc. Am.*, *92*, 1433–1442, doi:10.1785/0120000908.

Jarchow, C. M., G. A. Thompson, R. D. Catchings, and W. D. Mooney (1993), Seismic evidence for active magmatic underplating beneath the Basin and Range province, western United States, *J. Geophys. Res.*, *98*, 22,095–22,108, doi:10.1029/93JB02021.

Kirby, S. H., and A. K. Kronenberg (1987), Rheology of the lithosphere; selected topics, *Rev. Geophys.*, *25*, 1219–1244, doi:10.1029/RG025i006p01219.

Lachenbruch, A. H., J. H. Sass, and S. P. Galanais (1985), Heat flow in southernmost California and the origin of the Salton Trough, *J. Geophys. Res.*, *90*, 6709–6736, doi:10.1029/JB090iB08p06709.

Langbein, J., D. Hill, T. Parker, and S. Wilkinson (1995), Shallow and peripheral volcanic sources of inflation revealed by modeling two-color geodimeter and leveling data from Long Valley caldera, California, 1988–1992, *J. Geophys. Res.*, *100*, 12,487–12,495, doi:10.1029/95JB01052.

Larsen, S., R. Reilinger, and L. Brown (1986), Evidence of ongoing crustal deformation related to magmatic activity near Socorro, New Mexico, *J. Geophys. Res.*, *91*, 6283–6292, doi:10.1029/JB091iB06p06283.

Laube, N., and J. Springer (1998), Crustal melting by ponding of mafic magmas: A numerical model, *J. Volcanol. Geotherm. Res.*, *81*, 19–35, doi:10.1016/S0377-0273(97)00072-3.

Lister, J. R., and R. C. Kerr (1991), Fluid-mechanical models of crack propagation and their application to magma transport in dykes, *J. Geophys. Res.*, *96*, 10,049–10,077, doi:10.1029/91JB00600.

Matzel, J. E. P., S. A. Bowring, and R. B. Miller (2006), Time scales of pluton construction at differing crustal levels: Examples from the Mount Stuart and Tenpeak intrusions, North Cascades, Washington, *Geol. Soc. Am. Bull.*, *118*, 1412–1430, doi:10.1130/B25923.1.

McMillan, N. J., A. P. Dickin, and D. Haag (2000), Evolution of magma source regions in the Rio Grande Rift, southern New Mexico, *Geol. Soc. Am. Bull.*, *112*, 1582–1593, doi:10.1130/0016-7606(2000)112<1582:EOMSRI>2.0.CO;2.

Mohr, P. (1992), Nature of the crust beneath magmatically active continental rifts, *Tectonophysics*, *213*, 269–284, doi:10.1016/0040-1951(92)90263-6.

Mooney, W. D., and T. M. Brocher (1987), Coincident seismic reflection/refraction studies of the continental lithosphere: a global review, *Geophys. J. R. Astron. Soc.*, *89*, 1–6.

Nelson, K., et al. (1996), Partially molten middle crust beneath southern Tibet: Synthesis of project INDEPTH results, *Science*, *274*, 1684–1688, doi:10.1126/science.274.5293.1684.

Newman, A. V., T. H. Dixon, and N. Gourmelen (2006), A four-dimensional viscoelastic deformation model for Long Valley Caldera, California, between 1995 and 2000, *J. Volcanol. Geotherm. Res.*, *150*, 244–269, doi:10.1016/j.jvolgeores.2005.07.017.

Parker, E. C., et al. (1984), Upwarp of anomalous asthenosphere beneath the Rio Grande Rift, *Nature*, *312*, 354–356, doi:10.1038/312354a0.

Parsons, T., N. H. Sleep, and G. A. Thompson (1992), Host rock rheology controls on the emplacement of tabular intrusions: Implications for

underplating of extended crust, *Tectonics*, *11*, 1348–1356, doi:10.1029/92TC01105.

Paterson, S., and T. Fowler (1993), Reexamining pluton emplacement processes, *J. Struct. Geol.*, *15*, 191–206, doi:10.1016/0191-8141(93)90095-R.

Petford, N., A. Cruden, K. McCaffrey, and J. Vigneresse (2000), Granite magma formation, transport and emplacement in the Earth's crust, *Nature*, *408*, 669–673, doi:10.1038/35047000.

Pollitz, F. F., C. Wicks, and W. Thatcher (2001), Mantle flow beneath a continental strike-slip fault: Postseismic deformation after the 1999 Hector Mine earthquake, *Science*, *293*, 1814–1818, doi:10.1126/science.1061361.

Ranalli, G. (1995), *Rheology of the Earth*, 2nd ed., Chapman and Hall, London.

Reilinger, R. E., and J. E. Oliver (1976), Modern uplift associated with a proposed magma body in the vicinity of Socorro, *N. M. Geol.*, *4*, 583–586.

Reiter, M. (2005), Subsurface temperatures and crustal strength changes within the seismogenic layer at Arroyo del Coyote in the Socorro seismic area, central Rio Grande Rift, New Mexico, *Geol. Soc. Am. Bull.*, *117*, 307–318, doi:10.1130/B25557.1.

Rinehart, E., and A. Sanford (1981), Upper crustal structure of the Rio Grande Rift near Socorro, New Mexico, from inversion of microearthquake S-wave reflections, *Bull. Seismol. Soc. Am.*, *71*, 437–450.

Rivet, D., and Y. Fialko (2007), Interseismic secular deformation in southern California from InSAR-derived maps over the time period between 1992 and 2006, *Eos Trans. AGU*, *88*, Abstract G51C-0620.

Ryan, M. P. (1993), Neutral buoyancy-controlled magma transport and storage in mid-ocean ridge magma reservoirs, *J. Geophys. Res.*, *98*, 22,321–22,338, doi:10.1029/93JB02394.

Ryan, M. P. (1994), Neutral buoyancy-controlled magma transport and storage in mid-ocean ridge magma reservoirs and their sheeted dike complex: a summary of basic relationships, in *Magmatic Systems*, edited by M. P. Ryan, pp. 97–138, doi:10.1016/S0074-6142(09)60094-2, Academic, San Diego, Calif.

Ryan, M. P., J. Y. K. Blevins, A. T. Okamura, and R. Y. Koyanagi (1983), Magma reservoir subsidence mechanics: Theoretical summary and application to Kilauea Volcano, Hawaii, *J. Geophys. Res.*, *88*(B5), 4147–4181, doi:10.1029/JB088iB05p04147.

Sanford, A. R., O. S. Alptekin, and T. R. Toppozada (1973), Use of reflection phases on microearthquake seismograms to map an unusual discontinuity beneath the Rio Grande Rift, *Bull. Seismol. Soc. Am.*, *63*, 2021–2034.

Savage, J. C., M. Lisowski, and W. H. Prescott (1985), Strain accumulation in the Rocky Mountain states, *J. Geophys. Res.*, *90*(B12), 10,310–10,320, doi:10.1029/JB090iB12p10310.

Schmidt, D., and R. Bürgmann (2003), Time-dependent land uplift and subsidence in the Santa Clara valley, California, from a large interferometric synthetic aperture radar data set, *J. Geophys. Res.*, *108*(B9), 2416, doi:10.1029/2002JB002267.

Sisson, T. W., K. Ratajeski, W. B. Hankins, and A. F. Glazner (2005), Voluminous granitic magmas from common basaltic sources, *Contrib. Mineral. Petrol.*, *148*, 635–661, doi:10.1007/s00410-004-0632-9.

Stankova, J., S. L. Bilek, C. A. Rowe, and R. C. Aster (2008), Characteristics of the October 2005 microearthquake swarm and reactivation of similar event seismic swarms over decadal time periods near Socorro, New Mexico, *Bull. Seismol. Soc. Am.*, *98*(1), 93–105, doi:10.1785/0120070108.

Wu, P. (2001), Postglacial induced surface motion and gravity in Laurentia for uniform mantle with power-law rheology and ambient tectonic stress, *Earth Planet. Sci. Lett.*, *186*, 427–435, doi:10.1016/S0012-821X(01)00258-8.

Yoshino, T., and T. Okudaira (2004), Crustal growth by magmatic accretion constrained by metamorphic P-T paths and thermal models of the Kohistan Arc, NW Himalaya, *J. Petrol.*, *45*, 2287–2302, doi:10.1093/petrology/egh056.

Yuan, X., et al. (2000), Subduction and collision processes in the Central Andes constrained by converted seismic phases, *Nature*, *408*, 958–961, doi:10.1038/35050073.

Y. Fialko and J. Pearse, Institute of Geophysics and Planetary Physics, Scripps Institution of Oceanography, University of California, San Diego, 9500 Gilman Dr., La Jolla, CA 92093-0225, USA. (jpearse@ucsd.edu)